



**Providing Choice & Value**  
Generic CT and MRI Contrast Agents

**FRESENIUS  
KABI**

CONTACT REP

**AJNR**

## **Longitudinal Whole-Brain N-Acetylaspartate Concentration in Healthy Adults**

D.J. Rigotti, I.I. Kirov, B. Djavadi, N. Perry, J.S. Babb and O. Gonen

*AJNR Am J Neuroradiol* 2011, 32 (6) 1011-1015

doi: <https://doi.org/10.3174/ajnr.A2452>

<http://www.ajnr.org/content/32/6/1011>

This information is current as of July 17, 2025.

# ORIGINAL RESEARCH

D.J. Rigotti  
I.I. Kirov  
B. Djavadi  
N. Perry  
J.S. Babb  
O. Gonen



## Longitudinal Whole-Brain *N*-Acetylaspartate Concentration in Healthy Adults

**BACKGROUND AND PURPOSE:** Although NAA is often used as a marker of neural integrity and health in different neurologic disorders, the temporal behavior of WBNA is not well characterized. Our goal therefore was to establish its normal variations in a cohort of healthy adults over typical clinical trial periods.

**MATERIALS AND METHODS:** Baseline amount of brain NAA,  $Q_{NAA}$ , was obtained with nonlocalizing proton MR spectroscopy from 9 subjects (7 women, 2 men;  $31.2 \pm 5.6$  years old).  $Q_{NAA}$  was converted into absolute millimole amount by using phantom-replacement. The WBNA concentration was derived by dividing  $Q_{NAA}$  with the brain parenchyma volume,  $V_B$ , segmented from MR imaging. Temporal variations were determined with 4 annual scans of each participant.

**RESULTS:** The distribution of WBNA levels was not different among time points with respect to the mean,  $12.1 \pm 1.5$  mmol/L ( $P > .6$ ), nor was its intrasubject change (coefficient of variation = 8.6%) significant between any 2 scans ( $P > .5$ ). There was a small (0.2 mL) but significant ( $P = .05$ ) annual  $V_B$  decline.

**CONCLUSIONS:** WBNA is stable over a 3-year period in healthy adults. It qualifies therefore as a biomarker for global neuronal loss and dysfunction in diffuse neurologic disorders that may be well worth considering as a secondary outcome measure candidate for clinical trials.

**ABBREVIATIONS:** CV = coefficient of variation; GM = gray matter;  $^1\text{H-MRS}$  = proton MR spectroscopy; MPRAGE = magnetization-prepared rapid acquisition of gradient echo; NAA = *N*-acetylaspartate;  $Q_{NAA}$  = absolute amount of NAA (millimoles); SNR = signal intensity-to-noise ratio;  $S_R$  = reference NAA peak area;  $S_S$  = subject NAA peak area; VOI = volume of interest;  $V_R^{180^\circ}$  = reference transmitter voltage;  $V_S^{180^\circ}$  = subject transmitter voltage; WBNA = whole-brain NAA concentration; WM = white matter

The biochemical information obtained from  $^1\text{H-MR}$  spectroscopy is often being combined with the anatomic information from conventional MR imaging to provide a more accurate snapshot of a variety of neurologic disorders.<sup>1-3</sup> This is done via the levels of several  $^1\text{H-MR}$  spectroscopy-detectable brain metabolites used as surrogate markers,<sup>4,5</sup> key among which is NAA, the second most abundant amino acid derivative in the mammalian brain.<sup>6-8</sup> Due to its near-exclusive localization to neurons and their processes, NAA is regarded as a marker for their health and density,<sup>9</sup> and its level has been reported to decline in all neurodegenerative central nervous system disorders in adults.<sup>10,11</sup>

Due to the chronic nature of these diseases, they are often studied serially.<sup>12-14</sup> The cost and complexity of such studies in humans, however, frequently limit their duration to a few years, with many months between samples.<sup>15</sup> Because the NAA level in healthy subjects is the implicit reference for the  $^1\text{H-MR}$  spectroscopy component of such studies, it is important to establish its temporal course in that population. This is

typically done, out of convenience, by cross-sectional averaging, with the assumption of neurologic stability.<sup>16,17</sup>

Small single-voxel, or 2D multivoxel VOIs located over the MR imaging-visible pathology are suited for  $^1\text{H-MR}$  spectroscopy studies of focal diseases.<sup>18-20</sup> Even the 3D MR spectroscopic imaging methods that are recently becoming more prevalent, especially for diffuse or multifocal disorders, rarely cover >50% of the brain. Due to their restricted coverage, these techniques require image guidance that subjects them to several intrinsic limitations, albeit less so than smaller VOI studies: 1) they must assume that changes occur only at MR imaging-visible pathologies; 2) although registration programs are available, misregistration errors can still confound serial studies; and 3) to eliminate lipid contamination from bone marrow and subcutaneous adipose tissue, cortical areas must be avoided or examined separately and with smaller VOIs, which can be time- and labor-intensive.<sup>21</sup> Fortunately, WBNA quantification, a short, simple, and easily implemented sequence, addresses all of these issues by providing global concentration (at a cost of localization). It has been shown to decrease cross-sectionally in several diffuse brain disorders while remaining stable in controls, as reviewed recently.<sup>22</sup>

Although cross-sectional reproducibility is a necessary condition for WBNA to be used as a surrogate marker for widespread neural loss in diffuse neurologic diseases, it is by itself insufficient. To attain that utility, the normal temporal variations in the healthy brain also must be established. Thus, here we report on the WBNA concentrations obtained both

Received September 21, 2010; accepted after revision October 26.

From the Department of Radiology, New York University School of Medicine, New York, New York.

This research was supported by National Institutes of Health grants EB01015 and NS050520.

Please address correspondence to Oded Gonen, PhD, Department of Radiology, New York University School of Medicine, 660 First Ave, 4th Floor, New York, NY 10016; e-mail: oded.gonen@med.nyu.edu



Indicates open access to non-subscribers at [www.ajnr.org](http://www.ajnr.org)

DOI 10.3174/ajnr.A2452

cross-sectionally and serially with annual scans in a cohort of healthy individuals over 3 years from baseline.

## Materials and Methods

### Human Subjects

Nine healthy subjects (7 women, 2 men;  $31.2 \pm 5.6$  years old [range, 24–43 years]) were recruited for this study. Their “healthy” status was based on negative answers to a questionnaire listing 28 neurologic disorders before the examination and an MR imaging deemed “unremarkable” by a neuroradiologist afterward. MR imaging and WB-NAA were performed on each subject at enrollment and 12, 24, and 36 months afterward. All gave Institutional Review Board–approved written informed consent, and the study was Health Insurance Portability and Accountability Act compliant.

### MR Imaging: Brain Volumetry

All experiments were done in a 3T whole-body MR scanner (Trio; Siemens, Erlangen, Germany) by using a TEM3000 circularly polarized transmit-receive head-coil (MRInstruments, Minneapolis, Minnesota). After each subject’s placement head-first supine into the magnet, we used a chemical shift imaging–based automatic shim procedure to adjust the scanner’s first and second order shims to a consistent  $27 \pm 3$  Hz full width at half maximum whole-head water line width in 3–5 minutes.<sup>23</sup> Sagittal T1-weighted MPAGE: TE/TR/TI = 2.6/1360/800 ms; 160 sections, 1.0 mm thick each, over a  $256 \times 256$ -mm<sup>2</sup> FOV with a  $256 \times 256$  matrix, followed for brain tissue volume,  $V_B$ , estimation. GM, WM, and CSF were segmented from the MPAGE images by using SPM2 segmentation (Wellcome Department of Cognitive Neurology, Institute of Neurology, London, United Kingdom).<sup>24,25</sup> The resultant probabilistic GM and WM “masks” for each section were summed on a pixel-by-pixel basis by using our in-house software to yield  $V_B$ .

### MR Spectroscopy: WBNA Quantification

The whole-head <sup>1</sup>H spectrum was obtained by using a nonlocalizing TE/TI/TR = 0/0.94/10-second sequence,<sup>26</sup> where the role of the long TR  $\gg$  T1 and short TE  $\approx$  0 is to ensure insensitivity to possible regional T1 and T2 variations, which are typically unknown, especially in pathologies. The subject’s whole-head <sup>1</sup>H spectrum was phased manually by using an in-house IDL software (RSI, Boulder, Colorado), and the edges of the Lorentzian shape of the NAA peak were visually identified over the broad baseline of the macromolecules and other N-acetyl–bearing species that also resonate at 2.02 ppm.<sup>27</sup> The identified NAA peak area,  $S_S$ , was then integrated by the program, as shown in Fig 1. Six operators performed this task, each blinded to the other 5 operators. An operator’s result more than twice the SD from the group mean for that subject was rejected. If more than 2 were rejected, that set was deemed to be of insufficient quality and excluded. Otherwise, the 4–6 “good” results are averaged into  $\bar{S}$  and converted into absolute amounts,  $Q_{NAA}$ , by phantom replacement against a reference 3-L sphere of  $1.5 \times 10^{-2}$  moles of NAA in water by using subject and reference NAA peaks,  $S_S$  and  $S_R$ , as follows:<sup>26</sup>

$$1) \quad Q_{NAA} = 1.5 \times 10^{-2} \cdot \frac{\bar{S}_S}{S_R} \times \frac{V_S^{180^\circ}}{V_R^{180^\circ}} \text{ moles,}$$

where  $V_R^{180^\circ}$  and  $V_S^{180^\circ}$  are the transmitter voltages into 50  $\Omega$  for nonselective 1-ms 180° inversion pulses on the reference and subject, respectively, reflecting their relative coil loading.

It is noteworthy that although several brain metabolites are visible

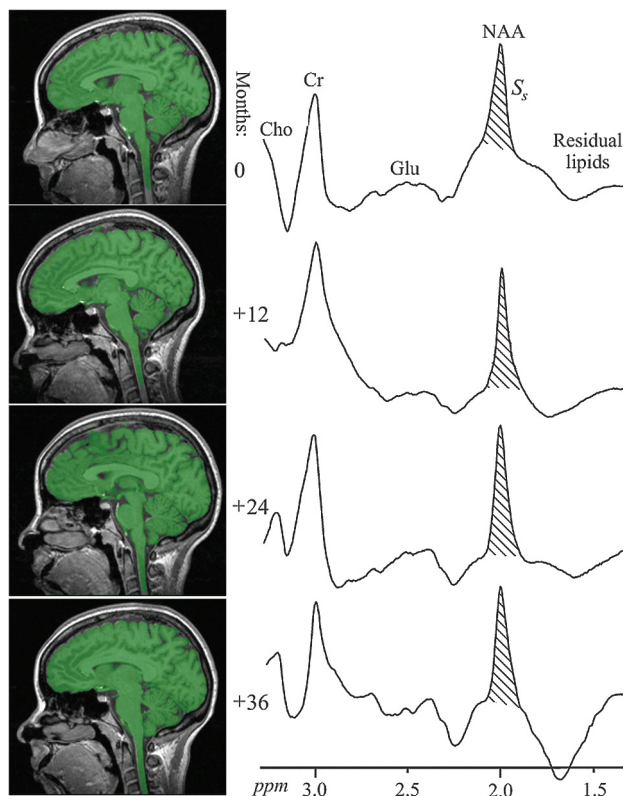


**Fig 1.** Left, Sample annual serial T1-weighted MPAGE images from the same subject overlaid with their brain parenchyma mask (green) obtained by using SPM2 segmentation. Note the mask correspondence with the underlying anatomy. Right, Serial whole-head <sup>1</sup>H-MR spectroscopy spectra from the same subject at baseline and 12, 24, and 36 months later. Note the high SNR in this spectrum, despite a short 2.6-minute acquisition (due to the large volume) and the similarities among the 4 serial spectra, despite minor shimming differences; more importantly, note that the peak areas,  $S_S$ , are all within  $\pm 7\%$ . Also note that although other brain metabolites are also visible in the spectra, eg, choline (Cho), glutamate (Glu), and creatine (Cr), only the NAA is implicitly localized to the brain by its biochemistry due to the nonlocalizing sequence used.

in the whole-head spectrum (Fig 1), only the NAA is implicitly localized by its biochemistry exclusively to neuronal cells, ie, to just the brain.<sup>28,29</sup> The presence of other metabolites (eg, creatine, choline, glutamate) in all other tissue types precludes determining the brain’s contribution to their signal intensity.

To account for natural brain size variations, the global NAA concentration, a specific metric independent of brain size, and therefore suitable for cross-sectional comparison, was used:

$$2) \quad \text{WBNA} = Q_{NAA}/V_B \text{ mM.}$$

Its intra- and intersubject variability has been shown previously at better than  $\pm 7\%$ .<sup>21,26,30</sup>

### Statistical Analyses

Mixed model analysis of variance was used to compare time points with respect to the intersubject mean of WBNA and  $V_B$ . WBNA and  $V_B$  were used as dependent variables in separate analyses, with time included in the model as a classification factor. The error variance was allowed to differ across time points to avoid the unnecessary assumption of variance homogeneity. Mixed model regression was used to estimate the rate of change in WBNA and  $V_B$  over time for each individual subject as well as the mean rate of change for the entire group. For all mixed model analyses, an autoregressive correlation structure was used to account for statistical dependencies among the

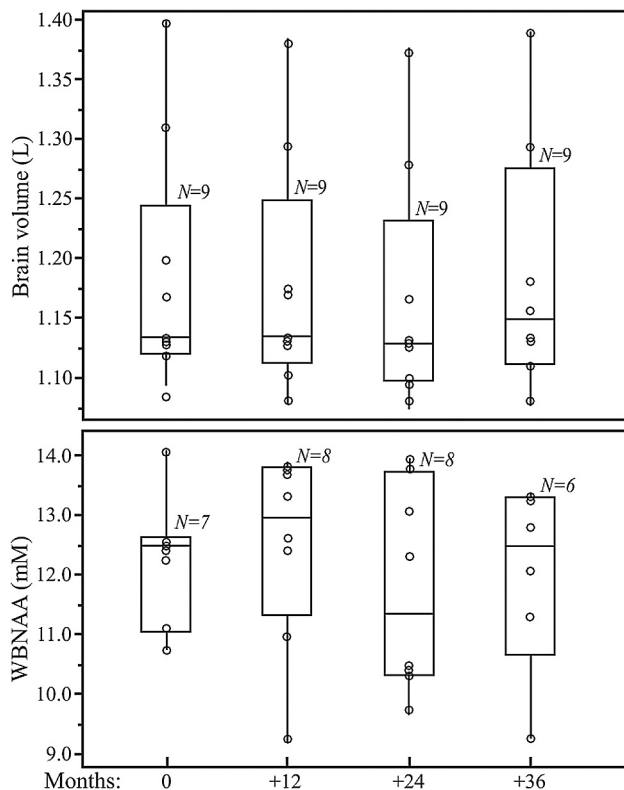


**Fig 2.** Boxplots showing the first, second (median), and third quartiles (box)  $\pm 95\%$  (whiskers) of  $V_B$  (top) and WBNA (bottom) distributions at baseline and 12, 24, and 36 month follow-ups. Open circles (○) on each boxplot represent the individual subject's values for each metric at that time point. Note that all 4 WBNA distributions are statistically indistinguishable ( $P > .5$ ), whereas the  $V_B$  values exhibit a small but significant group decline ( $P = .05$ ).

longitudinal observations recorded for each subject. That is, observations were assumed correlated only when acquired from the same subject and the strength of correlation between 2 observations was inversely related to the time between them.

Restricted maximum likelihood estimation of variance components in a random effects model was used to estimate the intrasubject and intersubject variance components of WBNA. These estimates were used to compute the intrasubject and intersubject CV as the square root of the relevant variance component expressed as a percentage of the overall mean of WBNA.

The estimated between- and within-subject variance components and the observed correlation between longitudinal measures on a subject were used to compute the precision that can be expected when the yearly rate of WBNA change is estimated by using a linear mixed model regression analysis over  $K$  equally spaced annual time points over 4 or 6 years for each of  $N$  subjects. The computation was based on the assumption that correlation between consecutive WBNA assessments is a nonincreasing function of the time between them; ie, they are more likely to be similar when taken closer together on a given person. This permitted a determination of the number of subjects that would be needed to detect any specific annual rate of WBNA change with either 80% or 90% statistical power at the 2-sided 5% significance level.

## Results

Sample whole-head brain  $^1\text{H}$  spectra from 4 time points of one subject: baseline and 12, 24, and 36 months are shown in Fig 1. Boxplots of the  $V_B$  and WBNA concentrations of the entire

**Table 1: Estimated sample sizes for 80% or 90% power at the 2-sided 5% significance level to detect specific yearly rates of WBNA change using  $K$  equally spaced annual scans**

Yearly WBNA Rate of Change (%)	80% Power		90% Power	
	$K = 4$	$K = 6$	$K = 4$	$K = 6$
2	207	104	276	139
4	54	28	71	37
6	25	14	33	18
8	15	9	20	11
10	11	7	14	8

cohort are shown in Fig 2. At each time point, 1 to 3 WBNA datasets were excluded (not consistently of the same subjects) due to failure of the quality criterion described above. Intra-subject  $V_B$ , shown in Fig 2, changed by an annual average of  $-0.2$  mL, which, though small in magnitude, represented a significant decline ( $P = .05$ ). WBNA, shown in Fig 2, exhibited similar mean NAA levels throughout, with average  $\pm$  SD of  $12.7 \pm 1.4$ ,  $12.9 \pm 1.9$ ,  $11.9 \pm 1.8$ , and  $12.2 \pm 2.1$  mmol/L at baseline and subsequent annual follow-ups. Its overall mean was  $12.1 \pm 1.5$  mmol/L, with an intersubject CV of 9.8%, similar to the  $\sim 10\%$  reported previously.<sup>31</sup>

The individual distribution of WBNA values at baseline was not significantly different from the follow-up points with respect to its mean ( $P > .6$ ), as shown in Fig 2. The intrasubject WBNA level did not change significantly over the course of the study (CV = 8.6%;  $P > .5$ ), nor did any individual's WBNA decrease significantly ( $P > .2$  for all). Based on the observed inter- and intrasubject variability mentioned above, Table 1 prescribes the number of subjects ( $N$ ) needed to be studied annually  $K$  times, to detect various annual %-WBNA change at either 80% or 90% statistical power. For example,  $n = 14$  subjects are needed to detect a 6% WBNA change, with  $K = 6$  equally spaced annual measurements at 80% power.

## Discussion

Quantitative MR metrics are now increasingly being used as biomarkers in clinical trials of neurologic disorders.<sup>32–35</sup> Among the various requirements described recently by Miller<sup>5</sup> of a biomarker for it to be considered as an “outcome measure” are its temporal reproducibility (in healthy control individuals) and by implication the conjugate metric—its sensitivity to significant change when applied to individual patients' disease progression or treatment response. Our goal therefore was to examine and quantify the intrasubject reproducibility of the WBNA method in a group of healthy individuals assumed to be stable in their global brain NAA concentration, and based on that metric, to also infer its sensitivity to temporal change.

The results obtained demonstrate WBNA's potential as a surrogate marker with respect to the reproducibility criterion. Specifically, that neural integrity, for which NAA is an accepted marker,<sup>36–38</sup> is statistically stable (as expected) in healthy individuals to within the intrinsic precision of the method,<sup>26</sup> over the course of 3 years, as shown in Fig 2. Because WBNA is normalized to  $V_B$ , stable to within  $\pm 0.25\%$ , as shown in Fig 2 and reported in the literature,<sup>39–41</sup> the inter- and intrasubject variabilities observed can be assigned entirely to  $Q_{\text{NAA}}$ ; ie, they reflect the biologic and instrumental “noise” of the spectroscopy part of the measurement.



The normal temporal variations in healthy young and middle-aged adults (range, 18–50 years old) at 1.5T were already reported in a study that was, however, subject to a higher dropout rate.<sup>42</sup> The present cohort was scanned more times (4 versus 2–3), and at a higher magnetic field (3T versus 1.5T), with less attrition (10% versus 50%), and at more regular time intervals (1 versus 2–3 years). The serial intrasubject variation observed in this study is similar to the 7%–11% reported previously<sup>42,43</sup> that in turn was similar to the ~6% obtainable with back-to-back scans.<sup>26</sup>

That the variations over a much longer time are of the same magnitude is another indication that they reflect the intrinsic precision of the method rather than real temporal fluctuations in an individual's brain physiology. This is further supported by the fact that the variations reported here at 3T are similar to those reported previously at 1.5T.<sup>26,42</sup> Because the WBNA sequence is “nonecho,” the NAA signal intensity suffers no T2-losses at either magnetic field; therefore, its (already high) SNR is doubled going from 1.5T to 3T. Because the SNR affects the measurement precision<sup>44</sup> and because a factor of  $\times 2$  improvement 1.5T to 3T makes negligible difference, this indicates that biologic variations and not measurement noise dominate the overall variability. The similarity of the serial to the cross-sectional variability of the WBNA suggests 1) that they reflect the intrinsic reproducibility of the method and 2) that within this approximately  $\pm 7\%$  precision, the global NAA concentration in the brains of healthy subjects is comparable and temporally stable.

The WBNA variations reported here potentially impact the design of studies that may use this metric as an outcome measure. Specifically, Table 1 determines the number of measurements, participants, and duration needed to detect a given magnitude of WBNA change. It also illustrates possible trade-offs in these parameters given the study designer's recruitment, cost, and duration constraints. It is noteworthy, eg, that to determine a 6% WBNA change, smaller than the 10%–20% reported for NAA in several neurologic disorders,<sup>12,45</sup> with 80% power requires 4 annual time points (3 years) when using 25 subjects, a number that is usually available in a single site. For the higher 90% statistical power that is often desirable in drug trials to reduce the risk of type II errors, the recruitment needs only rise to 33 subjects. Moreover, because it had been shown that, due to the use of absolute quantification, the WBNA distributions do not differ significantly among scanners,<sup>31</sup> recruitment across multiple sites is not likely to detract from the general utility of Table 1.

## References

- Lin AP, Tran TT, Ross BD. Impact of evidence-based medicine on magnetic resonance spectroscopy. *NMR Biomed* 2006;19:476–83
- Filippi M, Agosta F. Magnetic resonance techniques to quantify tissue damage, tissue repair, and functional cortical reorganization in multiple sclerosis. *Prog Brain Res* 2009;175:465–82
- Martinez-Bisbal MC, Celda B. Proton magnetic resonance spectroscopy imaging in the study of human brain cancer. *Q J Nuclear Med Mol Imaging* 2009;53:618–30
- Miller BL. A review of chemical issues in 1H NMR spectroscopy: N-acetyl-L-aspartate, creatine and choline. *NMR Biomed* 1991;4:47–52
- Miller DH. Biomarkers and surrogate outcomes in neurodegenerative disease: lessons from multiple sclerosis. *NeuroRx* 2004;1:284–94
- Birken DL, Oldendorf WH. N-acetyl-L-aspartic acid: a literature review of a compound prominent in 1H-NMR spectroscopic studies of brain. *Neurosci Biobehav Rev* 1989;13:23–31
- Baslow MH. Functions of N-acetyl-L-aspartate and N-acetyl-L-aspartylglutamate in the vertebrate brain: role in glial cell-specific signaling. *J Neurochem* 2000;75:453–59
- Baslow MH. Evidence that the tri-cellular metabolism of N-acetyl-L-aspartate functions as the brain's “operating system”: how NAA metabolism supports meaningful intercellular frequency-encoded communications. *Amino Acids* 2010;39:1139–45
- Benarroch EE. N-acetyl-L-aspartate and N-acetyl-L-aspartylglutamate: neurobiology and clinical significance. *Neurology* 2008;70:1353–57
- Danielsen EA, Ross B. *Magnetic Resonance Spectroscopy Diagnosis of Neurological Diseases*. New York: Marcel Dekker;1999
- Ross BD, Bluml S. Magnetic resonance spectroscopy of the human brain. *Anat Rec* 2001;265:54–84
- Schott JM, Frost C, Macmanus DG, et al. Short echo time proton magnetic resonance spectroscopy in Alzheimer's disease: a longitudinal multiple time point study. *Brain* 2010;133:3315–22
- Wild EJ, Fox NC. Serial volumetric MRI in Parkinsonian disorders. *Mov Disord* 2009;24(suppl 2):S691–98
- Sormani MP, Bruzzi P, Comi G, et al. MRI metrics as surrogate markers for clinical relapse rate in relapsing-remitting MS patients. *Neurology* 2002;58:417–21
- Filippi M, Grossman RI. MRI techniques to monitor MS evolution: the present and the future. *Neurology* 2002;58:1147–53
- Narayana PA, Doyle TJ, Lai D, et al. Serial proton magnetic resonance spectroscopic imaging, contrast-enhanced magnetic resonance imaging, and quantitative lesion volumetry in multiple sclerosis. *Ann Neurol* 1998;43:56–71
- Wolinsky JS, Narayana PA. Magnetic resonance spectroscopy in multiple sclerosis: window into the diseased brain. *Curr Opin Neurol* 2002;15:247–51
- Brooks WM, Friedman SD, Stidley CA. Reproducibility of 1H-MRS in vivo. *Magn Reson Med* 1999;41:193–97
- Marshall I, Wardlaw J, Cannon J, et al. Reproducibility of metabolite peak areas in 1H MRS of brain. *Magn Reson Imaging* 1996;14:281–92
- Bokde AL, Teipel SJ, Zebuhr Y, et al. A new rapid landmark-based regional MRI segmentation method of the brain. *J Neurol Sci* 2002;194:35–40
- Inglese M, Ge Y, Filippi M, et al. Indirect evidence for early widespread gray matter involvement in relapsing-remitting multiple sclerosis. *Neuroimage* 2004;21:1825–29
- Rigotti DJ, Inglese M, Gonen O. Whole-brain N-acetyl-L-aspartate as a surrogate marker of neuronal damage in diffuse neurologic disorders. *AJNR Am J Neuroradiol* 2007;28:1843–49
- Hu J, Javadi T, Arias-Mendoza F, et al. A fast, reliable, automatic shimming procedure using 1H chemical-shift-imaging spectroscopy. *J Magn Reson B* 1995;108:213–19
- Ashburner J, Friston K. Multimodal image coregistration and partitioning—a unified framework. *Neuroimage* 1997;6:209–17
- Ashburner J, Friston KJ. Voxel-based morphometry—the methods. *Neuroimage* 2000;11:805–21
- Gonen O, Viswanathan AK, Catalaa I, et al. Total brain N-acetyl-L-aspartate concentration in normal, age-grouped females: quantitation with non-echo proton NMR spectroscopy. *Magn Reson Med* 1998;40:684–89
- Behar KL, Rothman DL, Spencer DD, et al. Analysis of macromolecule resonances in 1H NMR spectra of human brain. *Magnetic Reson Med* 1994;32:294–302
- Baslow MH. N-acetyl-L-aspartate in the vertebrate brain: metabolism and function. *Neurochem Res* 2003;28:941–53
- Moffett JR, Ross B, Arun P, et al. N-Acetyl-L-aspartate in the CNS: from neurodiagnostics to neurobiology. *Prog Neurobiol* 2007;81:89–131
- Gonen O, Catalaa I, Babb JS, et al. Total brain N-acetyl-L-aspartate: a new measure of disease load in MS. *Neurology* 2000;54:15–19
- Benedetti B, Rigotti DJ, Liu S, et al. Reproducibility of the whole-brain N-acetyl-L-aspartate level across institutions, MR scanners, and field strengths. *AJNR Am J Neuroradiol* 2007;28:72–75
- Ciomas C, Montavont A, Rylvlin P. Magnetic resonance imaging in clinical trials. *Curr Opin Neurol* 2008;21:431–36
- Jack CR Jr, Slomkowski M, Gracon S, et al. MRI as a biomarker of disease progression in a therapeutic trial of milameline for AD. *Neurology* 2003;60:253–60
- Comi G, Filippi M. Clinical trials in multiple sclerosis: methodological issues. *Curr Opin Neurol* 2005;18:245–52
- Rovaris M, Filippi M. Magnetic resonance techniques to monitor disease evolution and treatment trial outcomes in multiple sclerosis. *Curr Opin Neurol* 1999;12:337–44
- Simmons ML, Frondoza CG, Coyle JT. Immunocytochemical localization of N-acetyl-L-aspartate with monoclonal antibodies. *Neuroscience* 1991;45:37–45
- Jenkins BG, Klivenyi P, Kustermann E, et al. Nonlinear decrease over time in N-acetyl-L-aspartate levels in the absence of neuronal loss and increases in glutamine and glucose in transgenic Huntington's disease mice. *J Neurochem* 2000;74:2108–19
- Jack CR Jr, Nambodiri MA, Cangro CB, et al. Immunohistochemical localization of N-acetyl-L-aspartate in rat brain. *Neuroreport* 1991;2:131–34
- Coffey CE, Wilkinson WE, Parashos IA, et al. Quantitative cerebral anatomy of

- the aging human brain: a cross-sectional study using magnetic resonance imaging. *Neurology* 1992;42:527–36
40. Pfefferbaum A, Mathalon DH, Sullivan EV, et al. A quantitative magnetic resonance imaging study of changes in brain morphology from infancy to late adulthood. *Arch Neurol* 1994;51:874–87
  41. Scallan RI, Frost C, Jenkins R, et al. A longitudinal study of brain volume changes in normal aging using serial registered magnetic resonance imaging. *Arch Neurol* 2003;60:989–94
  42. Rigotti DJ, Inglese M, Babb JS, et al. Serial whole-brain N-acetylaspartate concentration in healthy young adults. *AJNR Am J Neuroradiol* 2007;28:1650–51
  43. Hövener JB, Rigotti DJ, Amann A, et al. Whole-brain N-acetylaspartate MR spectroscopic quantification: performance comparison of metabolite versus lipid nulling. *AJNR Am J Neuroradiol* 2008;29:1441–45
  44. Greco JB, Sakaie KE, Aminipour S, et al. Magnetic resonance spectroscopy: an in vivo tool for monitoring cerebral injury in SIV-infected macaques. *J Med Primatol* 2002;31:228–36
  45. Filippi M, Bozzali M, Rovaris M, et al. Evidence for widespread axonal damage at the earliest clinical stage of multiple sclerosis. *Brain* 2003;126:433–37